Biogeosciences Discuss., https://doi.org/10.5194/bg-2017-551
Manuscript under review for journal Biogeosciences
Discussion started: 8 January 2018

Seasonal development of iron limitation in the sub-Antarctic zone

Thomas J. Ryan-Keogh[1,2], Sandy J. Thomalla[1,2], Thato N. Mtshali[1], Natasha R. van Horsten[1,3], Hazel Little[2]

[1]Southern Ocean Carbon and Climate Observatory, Natural Resources and Environment, CSIR, Rosebank, Cape Town, 7700, South Africa

[2]Department of Oceanography, University of Cape Town, Rondebosch, Cape Town, 7701, South Africa

[3]Department of Earth Sciences, Stellenbosch University, Stellenbosch, 7600, South Africa

Correspondence to: tryankeogh@csir.co.za

Abstract

The seasonal and sub-seasonal dynamics of iron availability within the sub-Antarctic zone (SAZ, ~40 – 45°S) play an important role in the distribution, biomass and productivity of the phytoplankton community. The variability in iron availability is due to an interplay between winter entrainment, diapycnal diffusion, storm-driven entrainment, iron scavenging and iron recycling processes. Biological observations utilising grow-out iron addition incubation experiments were performed at different stages of the seasonal cycle within the SAZ to determine the importance of these supply mechanisms. Here we demonstrate that at the beginning of the growing season there is sufficient iron to meet the demands of the phytoplankton community, but as the growing season develops the supply mechanisms fail to meet this demand. Phytoplankton increase their photosynthetic efficiency and net growth rates

Biogeosciences Discuss., https://doi.org/10.5194/bg-2017-551
Manuscript under review for journal Biogeosciences
Discussion started: 8 January 2018

following iron addition from mid to late summer, with no differences determined during early summer; suggestive of seasonal iron depletion and low iron resupply. The result of which is residual macronutrients at the end of the growing season, and the prevalence of the high-nutrient low-chlorophyll (HNLC) condition. We conclude that despite the prolonged growing season characteristic of the SAZ, which can extend into late summer/early autumn, the results suggest that the iron supply mechanisms are insufficient to maintain potential maximal growth and productivity throughout the season.

Biogeosciences Discuss., https://doi.org/10.5194/bg-2017-551
Manuscript under review for journal Biogeosciences
Discussion started: 8 January 2018

1. Introduction

The Southern Ocean is an important region for atmospheric CO_2 drawdown, 30-40% of global anthropogenic carbon uptake (Khatiwala et al., 2009; Mikaloff Fletcher et al., 2006; Schlitzer, 2002), which is driven by phytoplankton community production and the biological carbon pump (BCP). The BCP is however sensitive to environmental influences that are associated with climate change, which include an intensification of the westerly winds (Le Quéré et al., 2009), and altered upwelling and mixed layer stratification (Bopp et al., 2005; Boyd, 2002). Together, these changes will impact the light and nutrient supply to the phytoplankton community, which could in turn alter the efficiency and extent of the BCP in the future.

The high productivity characteristic of this region is driven in part by the high macronutrient availability, while phytoplankton growth and productivity is ultimately constrained by the availability of light and iron (de Baar et al., 1990; Martin et al., 1990). The result of this limitation is the prevalence of macronutrients in the surface waters at the end of the growing season, resulting in the paradoxical high nutrient low chlorophyll (HNLC) conditions characteristic of the region. Further controls on the seasonal evolution and extent of the phytoplankton bloom include potential silicate limitation (Boyd et al., 2010; Hutchins et al., 2001), top-down controls by meso- and micro-zooplankton grazing (Dubischar and Bathmann, 1997; Moore et al., 2013; Pakhomov and Froneman, 2004; Smetacek et al., 2004) and seasonal/sub-seasonal changes in the critical and mixed layer depths (Fauchereau et al., 2011; Nelson and Smith, 1991).

Iron is a key component of photosynthesis due to the high requirements in the formation and function of key photosynthetic proteins, including photosystems I and photosystem II (Raven, 1990; Shi et al., 2007; Strzepek and Harrison, 2004). In addition, iron requirements by phytoplankton are closely linked to light availability, displaying an inverse relationship. Under

low light conditions phytoplankton can maximise photosynthesis in different ways; by either increasing the size of their photosynthetic units or by increasing the number of their photosynthetic units, the latter resulting in an increase in the iron requirements under low light (Maldonado et al., 1999; Raven, 1990; Strzepek et al., 2012; Strzepek et al., 2011; Sunda and Huntsman, 1997). This close coupling of light and iron that increases the cellular demand for iron under low light can diminish light dependent photosynthesis when iron concentrations are too low to support growth (Hiscock et al., 2008; Moore et al., 2013; Ryan-Keogh et al., 2017b). Iron is also required in the function of both nitrate and nitrite reductase (de Baar et al., 2005), which function to facilitate the assimilation of nitrate and nitrite and their subsequent intracellular reduction to ammonium. In the Southern Ocean, and other HNLC areas, nitrate uptake rates are reported as becoming iron limited for this reason (Cochlan, 2008; Lucas et al., 2007; Moore et al., 2013; Price et al., 1994). However, rather than iron limitation directly inhibiting nitrate/nitrite reductase activity the cause of reduced uptake rates may be the result of a bottleneck further downstream due to a lack of photosynthetically derived reductant (Milligan and Harrison, 2000). The result of this is the excretion of excess nitrate and nitrite back into the water column, culminating in the HNLC condition that prevails in the Southern Ocean.

The Atlantic sector of the Southern Ocean is composed of a series of water masses, each with distinct physical and chemical properties, that are constrained by circumpolar fronts with large geostrophic velocities (Nowlin and Klinck, 1986; Orsi et al., 1995). The differing physical and chemical properties create a high degree of zonal variability within the biology, in particular the timing and extent of phytoplankton seasonal blooms (Thomalla et al., 2011). Key physical controls on this variability include sea ice cover and day length, yet this is not enough to explain the full range of variability measured. An alternative approach has examined whether the supply mechanisms of iron to the mixed layer differ significantly in their extent

allowing regions like the sub-Antarctic zone (SAZ) to exhibit prolonged summer blooms in comparison to the polar front zone (PFZ) (Thomalla et al., 2011). Tagliabue et al. (2014) postulated that due to weak diapycnal inputs of iron there must be a heavy reliance of Fe-recycling within the mixed layer to meet the iron demand. An alternative hypothesis is that summer eddy-storm interactions sustain mixed layer biomass through entrainment, particularly in the SAZ (Carranza and Gille, 2015; Nicholson et al., 2016; Swart et al., 2015). As a storm passes through the SAZ it deepens the mixed layer accessing the subsurface iron reservoir, the subsequent re-shoaling of this buoyant water fuels surface water phytoplankton growth in a high light environment. The drivers of the seasonal characteristics of these regions is likely a combination of both factors with variable dominance in time and space. Regardless, a greater understanding of the iron supply mechanisms and whether they meet the demand for phytoplankton growth is required.

This paper aims to test whether the phytoplankton community in the sub-Antarctic zone is seasonally limited by iron availability. This was done through a series of ship-board grow-out nutrient addition incubation experiments were performed to determine the extent to which the addition of iron at different times of the growing season would relieve the phytoplankton from iron limitation driving an increase photosynthetic efficiency, biomass and growth potential.

2. Materials and Methods

2.1. Oceanographic Sampling

The samples and data presented here were obtained during the annual Austral summer relief voyage of the South African National Antarctic Expedition 55 (SANAE 55) onboard the S.A.

Agulhas II to the Atlantic sector of the Southern Ocean as part of the Southern Ocean Seasonal Cycle Experiment III (SOSCEx III, (Swart et al., 2012)); from the 3rd December 2015 to 11th February 2016. During the cruise, 3 long-term (144 - 168 h) nutrient addition incubation experiments were performed within the sub-Antarctic zone of the Atlantic sector of the Southern Ocean (Fig. 1) to determine whether relief from iron limitation drove changes in phytoplankton photophysiology and biomass (Table). Uncontaminated whole seawater was collected from 30 - 35 m depth in Teflon-lined, external closure 12 L Go-Flo samplers deployed on a trace metal clean CTD rosette system.

2.2. Nutrient addition incubation experiments

Nutrient addition incubation experiments were performed using methods similar to those employed previously in the Southern Ocean (Moore et al., 2007; Nielsdóttir et al., 2012; Ryan-Keogh et al., 2017a) and the high latitude North Atlantic (Ryan-Keogh et al., 2013). Water for experiments were allowed to settle in the Go-Flo samplers before being transferred unscreened into acid-washed 50 L LDPE carboy (Thermo scientific) to ensure homogenization; the homogenized water was then redistributed unscreened into 2.4 L polycarbonate bottles (Nalgene) for the experiments. The triplicate initial samples were collected from the same 50L LDPE carboy. Experiments during the cruise were incubated under two treatments, control and iron addition (2.0 nM $FeCl_3$, 'Fe'), at a constant screened (LEE filters) light level of 129.45 µmol quanta m^{-2} s^{-1}. Light levels were determined using a handheld 4π PAR sensor (Biospherical Instruments), and were set on a day:night cycle according to the *in situ* sunset/sunrise times. All experimental incubations were conducted as biological duplicates or triplicates. Temperature was set at the in situ collection temperature for all samples. All bottle tops were externally sealed with film (Parafilm), and bottles were double bagged with clear

polyethylene bags to minimize risks of contamination during the incubation. Subsampling of all experiments occurred at the same time of day as the initial set-up.

2.3. Chlorophyll a and Nutrient Analysis

Samples for chlorophyll-a (Chl) analysis, 250 mL, were filtered onto GF/F filters and then extracted into 90% acetone for 24 h in the dark at -20°C, followed by analysis with a fluorometer (TD70; Turner Designs) (Welschmeyer, 1994). Macronutrient samples were drawn into 50 mL diluvials and stored at -20°C until analysis on land. Nitrate + Nitrite and Silicate were measured using a Lachat Flow Injection Analyser (Egan, 2008; Wolters, 2002), whilst Nitrite and Phosphate were determined manually by colorimetric method as specified by Grasshoff et al. (1983). Dissolved iron samples (DFe) were carefully collected in acid-washed 125 mL LDPE bottles, acidified with 30% HCl suprapur to pH ~1.7 (using 2 mL L^{-1} criteria) and stored at room temperature until analysis on land at UniBrest in France using the Chemiluminescence – Flow Injection Analyser (CL-FIA) method (Obata et al., 1993; Sarthou et al., 2003). Accuracy and precision of the method was verified by analysis of in-house internal standards and SAFe reference seawater samples (Johnson et al., 2007); the limits of detection were in order of 10 pM.

2.4. Phytoplankton Photosynthetic Physiology

Variable chlorophyll fluorescence was measured using a Chelsea Scientific Instruments FastOcean fast repetition rate fluorometer (FRRf) integrated with a FastAct laboratory system. Samples were acclimated in dark bottles at *in situ* temperatures, and FRRf measurements were blank corrected using carefully prepared 0.2 µm filtrates for all samples (Cullen and Davis,

158 2003). Protocols for FRRf measurements consisted of the following: 100 × 2 µs saturation
159 flashlets with a 2 µs interval, followed by 25 × 1 µs relaxation flashlets with an interval of 84
160 µs with a sequence interval of 100 ms. Sequences were repeated 32 times resulting in an
161 acquisition length of 3.2 s. The power of the excitation LED (λ450) was adjusted between
162 samples to saturate the observed fluorescence transients within a given range of $R\sigma_{PSII}$ (the
163 probability of a reaction centre being closed during the first flashlet). $R\sigma_{PSII}$ was optimised
164 between 0.042 to 0.064 as per the manufacturer's specifications. By adopting this approach, it
165 ensures the best signal-to-noise ratio in the recovered parameters whilst accommodating
166 significant variations in the photophysiology of the phytoplankton community without having
167 to adjust the protocol. Data from the FRRf were analysed to derive the fluorescence parameters
168 as defined in Roháček (2002), by fitting transients to the model of Kolber et al. (1998).
169
170 **2.5. Phytoplankton Composition**
171
172 Pigment samples from the incubation experiments were collected by filtering 0.5 – 2.0 L of
173 water onto 25 mm GF/F filters. Filters were frozen and stored at -80°C until analysis in
174 Villefranche, France on a HPLC Agilent Technologies 1200. Filters were extracted in 100%
175 methanol, disrupted by sonification, clarified by filtration and analysed by HPLC following the
176 methods of Ras et al. (2008); limits of detection were on the order of 0.1 ng L^{-1}. Pigment
177 composition data were standardized through root square transformation before cluster analysis
178 utilizing multi-dimensional scaling, where similar samples appear together and dissimilar
179 samples do not. Samples were grouped and analysed in CHEMTAX (Mackey et al., 1996)
180 using the pigment ratios from Gibberd et al. (2013). Multiple iterations of pigment ratios were
181 used to reduce uncertainty in the taxonomic abundance as described in (Gibberd et al., 2013),
182 with the solution that had the smallest residual used for the estimated taxonomic abundance.

Biogeosciences Discuss., https://doi.org/10.5194/bg-2017-551
Manuscript under review for journal Biogeosciences
Discussion started: 8 January 2018

183

184 **2.6. Ancillary physical data**

185

186 Temperature and salinity profiles were obtained from a Sea-Bird CTD mounted on the rosette
187 system. The mixed layer depth was calculated following de Boyer Montégut et al. (2004),
188 where the temperature differs from the temperature at 10 m by more than 0.2°C (ΔT_{10m} =
189 0.2°C). The position of the fronts were determined using sea surface height (SSH) data from
190 maps of absolute dynamic topography (MADT) (Swart et al., 2010). The percentage euphotic
191 depth was calculated as a function of the natural log of *in situ* photosynthetically active
192 radiation (PAR) and the diffuse attenuation coefficient K_z.

193

194 **2.7. Glider Dataset**

195

196 Autonomous Seagliders (SG542 & SG543) were deployed in mooring mode in the sub-
197 Antarctic zone of the Southern Ocean (43°S 8.5°E) as part of SOSCEx III. SG543 was
198 deployed from 28 July 2015 to 8 December 2015, followed by SG542 which continued
199 sampling until 8 February 2016. The deployment of both gliders resulted in a continuous high-
200 resolution time series of 1832 profiles over 196 days, down to depths of 1000 m. The gliders
201 measured a suite of parameters including conductivity, temperature, pressure, PAR,
202 fluorescence and optical backscattering at two wavelengths (λ = 470 and 700). At the
203 deployment and retrieval of each glider cross-calibration CTD casts were performed (all within
204 3km and 4 h of each other), yielding independent inter-calibrations between glider sensors and
205 bottle samples of Chl. Glider fluorescence was corrected for quenching and converted to units
206 of Chl (mg m^{-3}) as described in Thomalla et al. (2017). Wind stress (N m^{-2}) data was collected

from a weather station mounted on a simultaneous deployment of a Liquid Robotics Wave Glider; wind stress was corrected to 10 m using the wind profile power-law (Irwin, 1967).

2.8. Data analysis

Sample means and standard deviations were calculated using Python, followed by tests for normality and equal variance prior to analysis of variance to determine treatment effects (SciPy v0.17.1, Python v3.6). Significant results are reported at the 95% confidence level ($p < 0.05$).

3. Results

The experiment set-up location in the SAZ spanned 66 days from the initiation of the first experiment to the initiation of the third experiment. Chlorophyll concentrations did not vary substantially between initiations, ranging from 0.84 – 0.97 μg L^{-1}, alongside no significant variations in temperature and salinity (Table 1). Silicate concentrations remained fairly constant between experiments, with concomitant decreases in phosphate and dissolved iron (DFe) concentrations; whereas nitrate concentrations increased throughout the growing season. Photophysiological measurements of quantum efficiency (F_v/F_m) ranged from 0.19 – 0.30 with decreases in the cross-section of PSII (σ_{PSII}) from 14.79 to 7.08 nm^{-2}. All experiments were set up with water collected from above the mixed layer and the mean euphotic depth of 63.89±19.13 m, with the percentage of surface light ranging from 14.83 – 10.66%.

Data from 144-168 h experiments in the SAZ indicated variable responses to iron addition to the extant phytoplankton community (Fig. 2). During 'early-summer' (experiment 1), no evidence for iron stress was observed as indicated in the similar responses in F_v/F_m (Fig. 2a) and chlorophyll (Fig. 2b) between iron addition (+ Fe) and control treatments; both variables

232 increased to similar values at the end time point. Statistical analysis confirmed that there were
233 no significant differences in F_v/F_m or chlorophyll. The effective cross-section of PSII (σ_{PSII}
234 (nm^{-2})) displayed a similar pattern with no significant differences between treatments,
235 decreasing in both treatments to 5.68±0.27 and 5.63±0.13 for the control and iron addition
236 treatments respectively. Experiment 2, initiated 28 days later in 'mid-summer', did exhibit
237 signs of potential iron limitation (Fig. 2c, 2d). F_v/F_m increased from 0.30±0.02 to maximum of
238 0.39±0.01 at 120 h, whilst the control treatment ranged between 0.27 and 0.34 (Fig. 2c).
239 Moreover, chlorophyll concentrations were over 2 times higher in the iron addition treatment
240 compared to the controls at the end time point (Fig. 2d). Significant differences were observed
241 for F_v/F_m from 72 h onwards and for chlorophyll concentrations from 120 h onwards. σ_{PSII}
242 decreased to a minimum of 4.62±0.15 nm^{-2} in the iron addition at 120 h, corresponding to the
243 highest value in F_v/F_m; whereas the control treatment decreased from 6.45±0.23 to 5.96±0.13
244 nm^{-2}. The final experiment in 'late-summer' (experiment 3) displayed similar evidence for
245 potential iron limitation within the extant phytoplankton community (Fig. 2e, f). F_v/F_m in the
246 control treatment remained constant at 0.26±0.01, whereas in the iron addition treatment it
247 increased to 0.33±0.01 (Fig. 2e). Chlorophyll concentrations were 2.5 times higher in the iron
248 addition treatment compared to the controls after 144 h (Fig. 2f), resulting in significant
249 differences in F_v/F_m from 24 h and in chlorophyll concentrations at the end time point. σ_{PSII}
250 also decreased to a greater extent than the control in experiment 3 from 7.08±0.48 nm^{-2} to a
251 minimum of 5.45±0.15 nm^{-2}, compared to 6.23±0.14 nm^{-2} in the control at 144 h.

252 Chlorophyll specific growth rates (μ^{Chl}) were calculated for each experiment (Table 2,
253 Supplementary Information Fig. S1), displaying significantly higher growth rates for the iron
254 addition treatment in experiments 2 and 3 by up to 50% and 63% respectively, with no
255 significant differences in experiment 1. Enhanced nitrate drawdown $\Delta(NO_3^-)$ was exhibited in
256 experiment 2 (Table 2), with rates approximately 4 times higher than the other experiments.

No enhanced drawdown of phosphate or silicate was exhibited in any of the experiments. Taxonomic abundance (Supplementary Information, Fig. S2), indicated that the dominant component of the community was Haptophytes (>40%) when all experiments were initiated. Experiment 1 displayed significant increases in Diatoms in both treatments, alongside a significant increase in Synechococcus in the control treatment. Experiments 2 and 3 displayed similar results with significant increases in Diatoms following iron addition, with reductions in the Haptophyte group.

F_v/F_m is derived from measurements and analysis of the fluorescence kinetics of the photosynthetic reaction centre photosystem II (PSII) and associated light-harvesting antenna proteins (Kolber and Falkowski, 1993). Understanding the mechanistic changes in F_v/F_m can provide information on how the phytoplankton community respond to different stress factors. Increases in F_v/F_m following iron enrichment do not appear to be the result of an increase in PSII efficiency (F_v), but rather due to decreases in F_m and F_o (Behrenfeld et al., 2006; Lin et al., 2016; Macey et al., 2014; Ryan-Keogh et al., 2017a). To determine these relative changes in photophysiology, the absolute difference in F_v/F_m between the control and iron addition bottles was calculated at 24 h, $\Delta(F_v/F_m)$ (Ryan-Keogh et al., 2013). $\Delta(F_v/F_m)$ in experiment 1 was indistinguishable from zero (Fig. 3a), whereas in experiment 2 and 3 it was consistently positive with values of 0.08±0.01 and 0.06±0.00 respectively. These responses were markedly similar to the absolute differences in growth rates (Fig. 3b), with significantly higher differences in experiments 2 and 3. The absolute changes in maximum fluorescence (F_m, Fig. 3c) and variable fluorescence (F_v, Fig. 3d) normalized to chlorophyll were calculated to determine the mechanistic response. Significant differences were determined for F_m Chl^{-1} in experiments 2 and 3, with no significant differences in F_v Chl^{-1} across any experiments.

4. Discussion

282

283 Photosynthesis in the Southern Ocean is considered to be limited in winter by low mean
284 irradiance, with net phytoplankton growth rates increasing rapidly following the onset of
285 stratification in spring (Sverdrup, 1953). Despite these high levels of productivity and growth,
286 complete macronutrient drawdown is not possible due primarily to constraints in the
287 availability of iron (Boyd et al., 2007; de Baar et al., 1990). Reasons for this growth limitation
288 include the high iron requirements of the photosynthetic apparatus (Raven et al., 1999; Shi et
289 al., 2007) particularly under low light conditions and a lack of iron sources (Duce and Tindale,
290 1991; Tagliabue et al., 2014). Phytoplankton blooms in the SAZ are characterized by high
291 inter-annual and intra-seasonal variability with an extended duration that sustains high
292 chlorophyll concentrations late into summer (Carranza and Gille, 2015; Swart et al., 2015;
293 Thomalla et al., 2011; Thomalla et al., 2015). The longevity of these blooms is unusual as Fe
294 limitation at this time of year is expected to be limiting growth (Boyd, 2002). To determine the
295 extent to which the availability of iron is restricting phytoplankton photosynthesis and biomass
296 accumulation in the SAZ, a series of grow-out nutrient addition incubation experiments were
297 performed during the austral summer of 2015/2016.

298 The nutrient addition experiments (Fig. 2) demonstrated the development of seasonal
299 iron limitation of the in situ phytoplankton population within the SAZ from early summer
300 (December) to late summer (February). Experiment 1, which was set up during the early
301 growing season did not display any significant differences between treatments with all
302 parameters changing comparatively between the iron addition and control (Fig. 2a, 2b). The
303 rapid increase in F_v/F_m in both treatments at 24 h is likely due to potential bottle effects i.e. a
304 change in the light environment. Experiment 2 displayed the greatest response to the addition
305 of iron with significantly different F_v/F_m (Fig. 2c), chlorophyll derived net growth rates (Fig.
306 S1) and nitrate drawdown rates (Table 2). Experiment 3 also continued this trend with

307 significantly higher F_v/F_m (Fig. 2e) and net growth rates in the iron addition treatment
308 compared to the control (Fig. S1). The addition of iron also resulted in community level
309 changes switching from haptophyte dominated communities to diatom dominated communities
310 (Fig. S2). However, it remains to be determined whether this is shift towards small diatoms or
311 large diatoms, as large diatoms would require an increased silicate concentration which is a
312 limiting macronutrient in this region (Hutchins et al., 2001). Irregardless, this community shift
313 suggestive of community specific iron quota requirements (Ryan-Keogh et al., 2017a; Strzepek
314 et al., 2012; Strzepek et al., 2011), which drive the composition of the extant phytoplankton
315 community in the SAZ. The increased responses with time are indicative of seasonal iron
316 limitation, similar to the high latitude North Atlantic (Ryan-Keogh et al., 2013), where
317 potential iron sources are depleted early in the growing season resulting in HNLC conditions
318 at the end of the growing season.

319 Mechanistic changes in F_v/F_m, i.e. $\Delta(F_v/F_m)$, are a useful proxy to determine the
320 potential physiological signal of iron limitation without any superimposing taxonomic signal
321 (Suggett et al., 2009). The derived variable $\Delta(F_v/F_m)$ was higher in experiments in 2 and 3 (Fig.
322 3a), with values consistent with studies from the North and South Atlantic and the Ross Sea
323 (Browning et al., 2014; Ryan-Keogh et al., 2017a; Ryan-Keogh et al., 2013), which correlated
324 well with the observed differences in net growth rates ($\Delta\mu^{Chl}$, Fig. 3b). Whilst no empirical
325 relationship should be inferred between measures of photophysiology and measures of growth
326 rates (Kruskopf and Flynn, 2006; Parkhill et al., 2001; Price, 2005), the observed correlation
327 between these two independent variables suggest that a biomass independent measure of
328 physiological iron stress, F_v/F_m, is likely accompanied by a significant repression of
329 phytoplankton growth rates. These experiments also provide insights into the mechanistic iron-
330 stress response of phytoplankton photophysiology, where increases in F_v/F_m following iron
331 addition are due to a reduction in the ratio of F_m Chl^{-1} rather than F_v Chl^{-1} (Fig. 3c, 3d). This in

agreement with similar observations made in the Ross Sea, the high latitude North Atlantic and equatorial Pacific (Behrenfeld et al., 2006; Lin et al., 2016; Macey et al., 2014; Ryan-Keogh et al., 2017a), all regions where the phytoplankton communities are subject to iron limitation. Elevated ratios of F_m Chl^{-1} are potentially indicative of an energetically-decoupled pool of chlorophyll that possess a higher fluorescence yield than PSII at F_m (Macey et al., 2014; Ryan-Keogh et al., 2017a; Ryan-Keogh et al., 2012; Schrader et al., 2011). These pools can be significant in iron limited regions with important implications for chlorophyll derived primary productivity estimates that can be overestimated as a result (Behrenfeld et al., 2006; Macey et al., 2014).

The seasonal development of iron stress in the SAZ is suggestive of a primary dominant iron source to the surface waters, winter entrainment, which is subsequently depleted by upper ocean biota and abiotic scavenging onto settling particles (Tagliabue et al., 2014). Although diapycnal diffusion resupplies the mixed layer from late spring onwards, its low rates cannot be reconciled with potential phytoplankton uptake (Tagliabue et al., 2014). Instead, Tagliabue et al. (2014) propose that biologically recycled iron within the mixed layer is the dominant mechanism for sustaining summertime blooms. However, there is now compelling evidence to suggest that storm events may also play a critical role in extending the duration of summertime production through intra-seasonal entrainment of dissolved iron from a subsurface reservoir (Carranza and Gille, 2015; Fauchereau et al., 2011; Swart et al., 2015; Thomalla et al., 2011). This mechanism was tested using a 1D biogeochemical model by Nicholson et al. (2016) whose results suggest that intra-seasonal mixed layer perturbations may offer relief from iron limitation in summer, particularly if there is sufficient subsurface vertical mixing beneath the surface mixed layer.

A SAZ glider study by Little et al. (in review) corroborated these findings with summer match ups in small-scale temporal variability (< 10 days) in wind stress, MLD and chlorophyll

that emphasise the interconnectedness between the physical drivers and their biological response. Despite the similarity in the scales of variability, no correlation was observed between MLD and chlorophyll, which is explained by the variable response that MLD adjustments drive i.e. dilution (a decrease in chlorophyll with increasing MLD) and growth (an increase in chlorophyll with increasing MLD in response to nutrient entrainment) (Fauchereau et al., 2011). Both these scenarios can be observed in the glider time series from this study (Fig. 4), where increased wind stress and deeper MLD's were associated with both reduced (15 – 29 December) and enhanced (29 January – 7 February) chlorophyll. Both of the summer experiments were set up during periods of low wind stress (<0.2 N m^{-2}) with shallow MLDs, which explains the positive response to iron relief observed in experiments 2 and 3. Worth noting is the time period between 10 January and 29 January where the SAZ experienced uncharacteristically low winds for an extended period of time that drove very shallow MLD's (~20 m) and the development of a subsurface chlorophyll bloom. During this period, mean chlorophyll concentrations in the mixed layer (~0.4 mg m^{-3}) were lower than the euphotic zone (~0.8 mg m^{-3}), indicative of an iron supply within the mixed layer that is not sufficient to meet phytoplankton demands (i.e. surface water iron recycling is insufficient to sustain summertime productivity).

The decreasing DFe concentrations from the experimental depths do appear to suggest that DFe may not be sufficient, but this may not be a good indicator of iron stress as any limiting nutrient would be expected to be severely depleted through biological uptake with a resultant ambient concentrations that would remain close to zero despite possible event scale supply (Ryan-Keogh et al., 2017a). Furthermore, precaution must be taken when investigating changes in chlorophyll concentrations, as chlorophyll is only a proxy for phytoplankton biomass (Behrenfeld et al., 2016; Bellacicco et al., 2016; Mignot et al., 2014; Westberry et al., 2008;

Westberry et al., 2016) and an increase in the average concentration over the euphotic zone may represent a chlorophyll packaging effect due to lower light levels at depth.

The short transient periods of increased wind stress thus appear to provide temporary relief from iron limitation, and when examined across the entire growing season can provide a significant source of iron. Whilst the chlorophyll concentrations in late summer do not reach the spring maximum, they remain approximately double the winter time average (~0.4 mg m^{-3}). However, the increase of in situ nitrate concentrations are suggestive of community level iron limitation, as iron limitation can reduce the availability of photosynthetic reductant for nitrate reduction which can lead to the excretion of excess nitrate back into the water column (Cochlan, 2008; Lucas et al., 2007; Milligan and Harrison, 2000; Moore et al., 2013; Price et al., 1994). Irrespective of the different supply mechanisms; winter-entrainment, storm driven entrainment, diapycnal diffusion or microbial regeneration, the iron supply to the mixed layer is not sufficient for phytoplankton primary production to completely drawdown all available macronutrients. Moreover, this seasonal iron limitation may not be the only cause of sub-maximal productivity rates as silicate can also potentially limit phytoplankton growth in this region (Boyd et al., 2010; Hutchins et al., 2001). However, the significant shifts to diatom from haptophyte communities (Fig. S2) within the experimental treatments following iron addition suggest that silicate limitation may only be secondary limiting factor.

The current study represents an analysis of the seasonal development of iron limitation in the SAZ, highlighting how a lack of sufficient iron supply relates to potential community iron limitation. This is important for understanding Fe demand by the biota given the climate-mediated variability in supply mechanisms (i.e. atmospheric deposition) (Mackie et al., 2008), mixed layer depths and sea-ice cover (Boyd et al., 2012), as well as phytoplankton phenology (Strzepek et al., 2012). The biogeochemical significance of the Southern Ocean, including the highly productive Atlantic sector, will increase with respect to climate change (Marinov et al.,

2006); particularly as the Southern Ocean is the only HNLC region where the cryosphere is critical to seasonal dynamics. Climate-mediated changes to iron supply will influence the overall extent of phytoplankton growth, macronutrient drawdown and ultimately the strength and efficiency of the biological carbon pump. However, the variations of supply in the seasonal cycle will also continue to play an important role in this ecological important oceanic region and warrant further investigation.

Acknowledgements

We would like to thank the South African National Antarctic Programme (SANAP) and the captain and crew of the SA Agulhas II for their professional support through the cruise. We would also like to thank the engineers and glider pilots from Sea Technology Services for their professional support. Ryan Cloete and Ryan Miltz were involved in water collection and experimental set up. This work was undertaken and supported through the CSIR's Southern Ocean Carbon and Climate Observatory (SOCCO) Programme (http://socco.org.za/). This work was supported by CSIR's Parliamentary Grant funding (SNA2011112600001) and the NRF SANAP grant (SNA14073184298).

References

Behrenfeld, M. J., O'Malley, R. T., Boss, E. S., Westberry, T. K., Graff, J. R., Halsey, K. H., Milligan, A. J., Siegel, D. A., and Brown, M. B.: Revaluating ocean warming impacts on global phytoplankton, Nature Climate Change, 6, 323-330, 10.1038/nclimate2838, 2016.

Behrenfeld, M. J., Worthington, K., Sherrell, R. M., Chavez, F. P., Strutton, P., McPhaden, M., and Shea, D. M.: Controls on tropical Pacific Ocean productivity revealed through nutrient stress diagnostics, Nature, 442, 1025-1028, 10.1038/nature05083, 2006.

Bellacicco, M., Volpe, G., Colella, S., Pitarch, J., and Santoleri, R.: Influence of photoacclimation on the phytoplankton seasonal cycle in the Mediterranean Sea as seen by satellite, Remote Sens Environ, 184, 595-604, 10.1016/j.rse.2016.08.004, 2016.

Bopp, L., Aumont, O., Cadule, P., Alvain, S., and Gehlen, M.: Response of diatoms distribution to global warming and potential implications: A global model study, Geophysical Research Letters, 32, L19606, 10.1029/2005GL023653, 2005.

Boyd, P. W.: Environmental factors controlling phytoplankton processes in the Southern Ocean, J Phycol, 38, 844-861, 10.1046/j.1529-8817.2002.t01-1-01203.x, 2002.

Boyd, P. W., Arrigo, K. R., Strzepek, R., and van Dijken, G. L.: Mapping phytoplankton iron utilization: Insights into Southern Ocean supply mechanisms, J Geophys Res, 117, C06009, 10.1029/2011JC007726, 2012.

Boyd, P. W., Jickells, T., Law, C. S., Blain, S., Boyle, E. A., Buesseler, K. O., Coale, K. H., Cullen, J. J., de Baar, H. J. W., Follows, M., Harvey, M., Lancelot, C., Levasseur, M., Owens, N. P. J., Pollard, R., Rivkin, R. B., Sarmiento, J., Schoemann, V., Smetacek, V., Takeda, S., Tsuda, A., Turner, S., and Watson, A. J.: Mesoscale iron enrichment experiments 1993-2005: Synthesis and future directions, Science, 315, 612-617, 10.1126/science.1131669, 2007.

447 Boyd, P. W., Strzepek, R., Fu, F. X., and Hutchins, D. A.: Environmental control of open-
448 ocean phytoplankton groups: Now and in the future, Limnol Oceanogr, 55, 1353-1376,
449 10.4319/lo.2010.55.3.1353, 2010.
450 Browning, T. J., Bouman, H. A., Moore, C. M., Schlosser, C., Tarran, G. A., Woodward, E.
451 M. S., and Henderson, G. M.: Nutrient regimes control phytoplankton ecophysiology in the
452 South Atlantic, Biogeosciences, 11, 463-479, 10.5194/bg-11-463-2014, 2014.
453 Carranza, M. M. and Gille, S. T.: Southern Ocean wind-driven entrainment enhances satellite
454 chlorophyll-a through the summer, Journal of Geophysical Research: Oceans, 120, 304-323,
455 10.1002/2014JC010203, 2015.
456 Cochlan, W. P.: Nitrogen Uptake in the Southern Ocean. In: Nitrogen in the Marine
457 Environment, Elsevier, Amsterdam, 2008.
458 Cullen, J. J. and Davis, R. F.: The blank can make a big difference in oceanographic
459 measurements, Limnology and Oceanography Bulletin, 12, 29-35, 10.1002/lob.200312229,
460 2003.
461 de Baar, H. J. W., Boyd, P. W., Coale, K. H., Landry, M. R., Tsuda, A., Assmy, P., Bakker, D.
462 C. E., Bozec, Y., Barber, R. T., Brezinski, M. A., Buesseler, K. O., Boyé, M., Croot, P. L.,
463 Gervais, F., Gorbunov, M. Y., Harrison, P. J., Hiscock, W. T., Laan, P., Lancelot, C., Law, C.
464 S., Levasseur, M., Marchetti, A., Millero, F. J., Nishioka, J., Nojiri, Y., van Oijen, T., Riebesell,
465 U., Rijkenberg, M. J. A., Saito, H., Takeda, S., Timmermans, K. R., Veldhuis, M. J. W., Waite,
466 A. M., and Wong, C. S.: Synthesis of iron fertilization experiments: From the iron age in the
467 age of enlightenment, J Geophys Res, 110, C09S16, 10.1029/2004JC002601, 2005.
468 de Baar, H. J. W., Buma, A. G. J., Nolting, R. F., Cadee, G. C., Jacques, G., and Treguer, P. J.:
469 On iron limitation of the Southern Ocean: Experimental observations in the Weddell and Scotia
470 Seas, Mar Ecol Prog Ser, 65, 105-122, 10.3354/meps065105, 1990.

471 de Boyer Montégut, C., Madec, G., Fischer, A. S., Lazar, A., and Iudicone, D.: Mixed layer
472 depth over the global ocean: an examination of profile data and a profile-based climatology, J
473 Geophys Res, 109, C12003, 10.1029/2004JC002378, 2004.
474 Dubischar, C. D. and Bathmann, U. V.: Grazing impacts of copepods and salps on
475 phytoplankton in the Atlantic sector of the Southern Ocean, Deep-Sea Research II, 44, 415-
476 433, 10.1016/S0967-0645(96)00064-1, 1997.
477 Duce, R. A. and Tindale, N. W.: Atmospheric Transport of Iron and Its Deposition in the
478 Ocean, Limnol Oceanogr, 36, 1715-1726, 10.4319/lo.1991.36.8.1715, 1991.
479 Egan, L.: QuickChem Method 31-107-04-1-C - Nitrate and/or Nitrite in brackish or seawater,
480 Lachat Instruments, Colorado, USA, 2008.
481 Fauchereau, N., Tagliabue, A., Bopp, L., and Monteiro, P. M. S.: The response of
482 phytoplankton biomass to transient mixing events in the Southern Ocean, Geophysical
483 Research Letters, 38, L17601, 10.1029/2011GL048498, 2011.
484 Gibberd, M.-J., Kean, E., Barlow, R., Thomalla, S., and Lucas, M.: Phytoplankton
485 chemotaxonomy in the Atlantic sector of the Southern Ocean during late summer 2009, Deep-
486 Sea Research I, 78, 70-78, 10.1016/j.dsr.2013.04.007, 2013.
487 Grasshoff, K., Ehrhardt, M., and Kremling, K.: Methods of seawater analysis, Verlag Chemie,
488 Wienheim, Germany, 1983.
489 Hiscock, M. R., Lance, V. P., Apprill, A. M., Johnson, Z., Bidigare, R. R., Mitchell, B. G.,
490 Smith, W. O. J., and Barber, R. T.: Photosynthetic maximum quantum yield increases are an
491 essential component of Southern Ocean phytoplankton iron response, Proc Natl Acad Sci U S
492 A, 105, 4775-4780, 10.1073/pnas.0705006105, 2008.
493 Hutchins, D. A., Sedwick, P. N., DiTullio, G. R., Boyd, P. W., Quéguiner, B., Griffiths, F. B.,
494 and Crossely, C.: Control of phytoplankton growth by iron and silicic acid availability in the

495 subantarctic Southern Ocean: Experimental results from the SAZ Project, J Geophys Res, 106,
496 31559-31572, 10.1029/2000JC000333, 2001.
497 Irwin, J. S.: A theoretical variation of the wind profile power-law exponent as a function of
498 surface roughness and stability, Atmos Environ, 13, 191-194, 10.1016/0004-6981(79)90260-
499 9, 1967.
500 Johnson, K. S., Elrod, V. A., Fitzwater, S. E., Plant, J., Boyle, E., Bergquist, B., Bruland, K.
501 W., Aguilar-Islas, A. M., Buck, K., Lohan, M. C., Smith, G. J., Sohst, B. M., Coale, K. H.,
502 Gordon, M., Tanner, S., Measures, C. I., Moffett, J., Barbeau, K. A., King, A., Bowie, A. R.,
503 Chase, Z., Cullen, J. J., Laan, P., Landing, W., Mendez, J., Milne, A., Obata, H., Doi, T.,
504 Ossiander, L., Sarthou, G., Sedwick, P. N., Van den Berg, S., Laglera-Baquer, L., Wu, J.-F.,
505 and Cai, Y.: Developing standards for dissolved iron in seawater, Eos, Transactions American
506 Geophysical Union, 88, 131-132, 10.1029/2007EO110003, 2007.
507 Khatiwala, S., Primeua, F., and Hall, T.: Reconstruction of the history of anthropogenic CO_2
508 concentrations in the ocean, Nature, 462, 346-349, 10.1038/nature08526, 2009.
509 Kolber, Z. S. and Falkowski, P. G.: Use of active fluorescence to estimate phytoplankton
510 photosynthesis in situ, Limnol Oceanogr, 38, 1646-1665, 10.4319/lo.1993.38.8.1646, 1993.
511 Kolber, Z. S., Prášil, O., and Falkowski, P. G.: Measurements of variable chlorophyll
512 fluorescence using fast repetition rate techniques: defining methodology and experimental
513 protocols, Biochim Biophys Acta, 1367, 88-106, 10.1016/S0005-2728(98)00135-2, 1998.
514 Kruskopf, M. and Flynn, K. J.: Chlorophyll content and fluorescence responses cannot be used
515 to gauge reliably phytoplankton biomass, nutrient status or growth rate, New Phytol, 169, 525-
516 536, 10.1111/j.1469-8137.2005.01601.x, 2006.
517 Le Quéré, C., Raupach, M. R., Canadell, J. G., Marland, G., Bopp, L., Ciais, P., Conway, T. J.,
518 Doney, S. C., Feely, R. A., Foster, P., Friendlingstein, P., Gurney, K., Houghton, R. A., House,
519 J. I., Huntingford, C., Levy, P. E., Lomas, M. R., Majkut, J., Metzl, N., Ometto, J. P., Peters,

520 G. P., Prentice, I. C., Randerson, J. T., Running, S. W., Sarmiento, J. L., Schuster, U., Sitch,
521 S., Takahashi, T., Viovy, N., van der Werf, G. R., and Woodward, F. I.: Trends in the sources
522 and sinks of carbon dioxide, Nature Geoscience, 2, 831-836, 10.1038/ngeo689, 2009.
523 Lin, H., Kuzimov, F. I., Park, J., Lee, S., Falkowski, P. G., and Gorbunov, M. Y.: The fate of
524 photons absorbed by phytoplankton in the global ocean, Science, 351, 264-267,
525 10.1126/science.aab2213, 2016.
526 Lucas, M., Seeyave, S., Sanders, R., Moore, C. M., Williamson, R., and Stinchcombe, M.:
527 Nitrogen uptake responses to a naturally Fe-fertilised phytoplankton bloom during the
528 2004/2005 CROZEX study, Deep-Sea Research II, 54, 2138-2173, 10.4319/lo.2007.52.6.2540,
529 2007.
530 Macey, A. I., Ryan-Keogh, T. J., Richier, S., Moore, C. M., and Bibby, T. S.: Photosynthetic
531 protein stoichiometry and photophysiology in the high latitude North Atlantic, Limnol
532 Oceanogr, 59, 1853-1864, 10.4319/lo.2014.59.6.1853, 2014.
533 Mackey, M. D., Mackey, D. J., Higgins, H. W., and Wright, S. W.: CHEMTAX - a program
534 for estimating class abundances from chemical markers: application to HPLC measurements
535 of phytoplankton, Mar Ecol Prog Ser, 144, 265-283, 10.3354/meps144265, 1996.
536 Mackie, D. S., Boyd, P. W., McTainsh, G. H., Tindale, N. W., Westberry, T. K., and Hunter,
537 K. A.: Biogeochemistry of iron in Australian dust: From eolian uplift to marine uptake,
538 Geochemistry, Geophysics, Geosystems, 9, Q03Q08, 10.1029/2007GC001813, 2008.
539 Maldonado, M. T., Boyd, P. W., Harrison, P. J., and Price, N. M.: Co-limitation of
540 phytoplankton growth by light and Fe during winter in the NE subarctic Pacific Ocean, Deep-
541 Sea Research II, 46, 2475-2485, 10.1016/S0967-0645(99)00072-7, 1999.
542 Marinov, I., Gnanadesikan, A., Toggweiler, J. R., and Sarmiento, J. L.: The Southern Ocean
543 biogeochemical divide, Nature, 441, 964-967, 10.1038/nature04883, 2006.

544 Martin, J. H., Gordon, R. M., and Fitzwater, S. E.: Iron in Antarctic waters, Nature, 345, 156-
545 158, 10.1038/345156a0, 1990.
546 Mignot, A., Claustre, H., Uitz, J., Poteau, A., D'Ortenzio, F., and Xing, X.: Understanding the
547 seasonal dynamics of phytoplankton biomass and the deep chlorophyll maximum in
548 oligotrophic environments: A Bio-Argo float investigation, Global Biogeochemical Cycles, 28,
549 856-876, 10.1002/2013GB004781, 2014.
550 Mikaloff Fletcher, S. E., Gruber, N., Jacobson, A. R., Doney, S. C., Dutkiewicz, S., Gerber,
551 M., Follows, M., Joos, F., Lindsay, K., Menemenlis, D., Mouchet, A., Müller, S. A., and
552 Sarmiento, J. L.: Inverse estimates of anthropogenic CO_2 uptake, transport, and storage by the
553 the ocean, Global Biogeochemical Cycles, 20, GB2002, 10.1029/2005GB002530, 2006.
554 Milligan, A. J. and Harrison, P. J.: Effects of non-steady-state iron limitation on nitrogen
555 assimilatory enzymes in the marine diatom Thalassiosira weissflogii (Bacillariophyceae), J
556 Phycol, 36, 78-86, 10.1046/j.1529-8817.2000.99013.x, 2000.
557 Moore, C. M., Mills, M. M., Arrigo, K. R., Berman-Frank, I., Bopp, L., Boyd, P. W., Galbraith,
558 E. D., Geider, R. J., Guieu, C., Jaccard, S. L., Jickells, T. D., La Roche, J., Lenton, T. M.,
559 Mahowald, N. M., Marañón, E., Marinov, I., Moore, J. K., Nakatsuka, T., Oschlies, A., Saito,
560 M. A., Thingstad, T. F., Tsuda, A., and Ulloa, O.: Processes and patterns of oceanic nutrient
561 limitation, Nature Geoscience, 6, 701-710, 10.1038/NGEO1765, 2013.
562 Moore, C. M., Seeyave, S., Hickman, A. E., Allen, J. T., Lucas, M. I., Planquette, H., Pollard,
563 R. T., and Poulton, A. J.: Iron-light interactions during the CROZet natural iron bloom and
564 EXport experiment (CROZEX) I: Phytoplankton growth and photophysiology, Deep-Sea
565 Research II, 54, 2045-2065, 10.1016/j.dsr2.2007.06.011, 2007.
566 Nelson, D. M. and Smith, W. O. J.: Sverdrup revisited: Critical depths, maximum chlorophyll
567 levels and the control of Southern Ocean productivity by the irradiance-mixing regime, Limnol
568 Oceanogr, 36, 1650-1661, 1991.

569 Nicholson, S.-A., Lévy, M., Llort, J., Swart, S., and Monteiro, P. M. S.: Investigation into the
570 impact of storms on sustaining summer primary productivity in the Sub-Antarctic Ocean,
571 Geophysical Research Letters, 43, 9192-9199, 10.1002/2016GL069973, 2016.
572 Nielsdóttir, M. C., Bibby, T. S., Moore, C. M., Hinz, D. J., Sanders, R., Whitehouse, M., Korb,
573 R., and Achterberg, E. P.: Seasonal and spatial dynamics of iron availability in the Scotia Sea,
574 Mar Chem, 130, 62-72, 10.1038/345156a0, 2012.
575 Nowlin, W. D. and Klinck, J. M.: The physics of the Antarctic Circumpolar Current, Reviews
576 of Geophysics, 24, 469-491, 10.1029/RG024i003p00469, 1986.
577 Obata, H., Karatani, H., and Nakayama, E.: Automated determination of iron in seawater by
578 chelating resin concentration and chemiluminescence detection, Anal Chem, 65, 1524-1528,
579 10.1021/ac00059a007, 1993.
580 Orsi, A. H., Whitworth III, T. W., and Nowlin, W. D.: On the meridional extent and front of
581 the Antarctic Circumpolar Current, Deep-Sea Research I, 42, 641-673, 10.1016/0967-
582 0637(95)00021-W, 1995.
583 Pakhomov, E. A. and Froneman, P. W.: Zooplankton dynamics in the eastern Atlantic sector
584 of the Southern Ocean during austral summer 1997/1998, Deep-Sea Research II, 51, 2599-
585 2616, 10.1016/j.dsr2.2000.11.001, 2004.
586 Parkhill, J., Maillet, G., and Cullen, J. J.: Fluorescence-based maximal quantum yield for PSII
587 as a diagnostic of nutrient stress, J Phycol, 37, 517-529, 10.1046/j.1529-
588 8817.2001.037004517.x, 2001.
589 Price, N. M.: The elemental stoichiometry and composition of an iron-limited diatom, Limnol
590 Oceanogr, 50, 1149-1158, 2005.
591 Price, N. M., Ahner, B. A., and Morel, F. M. M.: The equatorial Pacific Ocean: Grazer-
592 controlled phytoplankton populations in an iron-limited ecosystem, Limnol Oceanogr, 39, 520-
593 534, 10.4319/lo.1994.39.3.0520, 1994.

Ras, J., Claustre, H., and Uitz, J.: Spatial variability of phytoplankton pigment distributions in the Subtropical South Pacific Ocean: comparison between in situ and predicted data, Biogeosciences, 5, 353-369, 10.5194/bg-5-353-2008, 2008.

Raven, J. A.: Predictions of Mn and Fe use efficiencies of phototrophic growth as a function of light availability for growth and C assimilation pathway, New Phytol, 116, 1-18, 10.1111/j.1469-8137.1990.tb00505.x, 1990.

Raven, J. A., Evans, M. C., and Korb, R. E.: The role of trace metals in photosynthetic electron transport in O_2-evolving organisms, Photosynth Res, 60, 111-150, 10.1023/A:1006282714942, 1999.

Rio, M. H., Guinehut, S., and Larnicol, G.: New CNES-CLS09 global mean dynamic topography computed from the combination of GRACE data, altimetry, and in situ measurements, J Geophys Res, 116, C07018, 10.1029/2010JC006505, 2011.

Roháček, K.: Chlorophyll Fluorescence Parameters: The Definitions, Photosynthetic Meaning, and Mutual Relationships, Photosynthetica, 40, 13-29, 10.1023/A:1020125719386, 2002.

Ryan-Keogh, T. J., DeLizo, L. M., Smith, W. O., Jr., Sedwick, P. N., McGillicuddy, D. J., Jr., Moore, C. M., and Bibby, T. S.: Temporal progression of photosynthetic strategy by phytoplankton in the Ross Sea, Antarctica, Journal of Marine Systems, 166, 87-96, 10.1016/j.jmarsys.2016.08.014, 2017a.

Ryan-Keogh, T. J., Macey, A. I., Cockshutt, A. M., Moore, C. M., and Bibby, T. S.: The cyanobacterial chlorophyll-binding-protein IsiA acts to increase the *in vivo* effective absorption cross-section of photosystem I under iron limitation, J Phycol, 48, 145-154, 10.1111/j.1529-8817.2011.01092.x, 2012.

Ryan-Keogh, T. J., Macey, A. I., Nielsdóttir, M., Lucas, M. I., Steigenberger, S. S., Stinchcombe, M. C., Achterberg, E. P., Bibby, T. S., and Moore, C. M.: Spatial and temporal

development of phytoplankton iron stress in relation to bloom dynamics in the high-latitude North Atlantic Ocean, Limnol Oceanogr, 58, 533-545, 10.4319/lo.2013.58.2.0533, 2013.

Ryan-Keogh, T. J., Thomalla, S. J., Mtshali, T. N., and Little, H.: Modelled estimates of spatial variability of iron stress in the Atlantic sector of the Southern Ocean, Biogeosciences, 14, 3883-3897, 10.5194/bg-14-3883-2017, 2017b.

Sarthou, G., Baker, A. R., Blain, S., Achterberg, E. P., Boye, M., Bowie, A. R., Croot, P., Laan, P., de Baar, H. J. W., Jickells, T. D., and Worsfold, P. J.: Atmospheric iron deposition and sea-surface dissolved iron concentrations in the eastern Atlantic Ocean, Deep Sea Research Part I: Oceanographic Research Papers, 50, 1339-1352, 10.1016/S0967-0637(03)00126-2, 2003.

Schlitzer, R.: Carbon export fluxes in the Southern Ocean: results from inverse modeling and comparion with satellite-based estimates, Deep-Sea Research II, 49, 1623-1644, 10.4319/lo.1994.39.3.0520, 2002.

Schrader, P. S., Milligan, A. J., and Behrenfeld, M. J.: Surplus Photosynthetic Antenna Complexes Underlie Diagnostics of Iron Limitation in a Cyanobacterium, PLoS ONE, 6, e18753, 10.1371/journal.pome.0018753, 2011.

Shi, T., Sun, Y., and Falkowski, P. G.: Effects of iron limitation on the expression of metabolic genes in the marine cyanobacterium *Trichodesmium erythraeum* IMS101, Environmental Microbiology, 9, 2945-2956, 10.1111/j.1462-2920.2007.01406.x, 2007.

Smetacek, V., Assmy, P., and Henjes, J.: The role of grazing in structuring Southern Ocean pelagic ecosystems and biogeochemical cycles, Antarct Sci, 16, 541-558, 10.1017/S0954102004002317, 2004.

Strzepek, R. F. and Harrison, P. J.: Photosynthetic architecture differs in coastal and oceanic diatoms, Nature, 431, 689-692, 10.1038/nature02954, 2004.

641 Strzepek, R. F., Hunter, K. A., Frew, R. D., Harrison, P. J., and Boyd, P. W.: Iron-light
642 interactions differ in Southern Ocean phytoplankton, Limnol Oceanogr, 57, 1182-1200,
643 10.4319/lo.2012.57.4.1182, 2012.
644 Strzepek, R. F., Maldonado, M. T., Hunter, K. A., Frew, R. D., and Boyd, P. W.: Adaptive
645 strategies by Southern Ocean phytoplankton to lessen iron limitation: Uptake of organically
646 complexed iron and reduced cellular iron requirements, Limnol Oceanogr, 56, 1983-2002,
647 10.4319/lo.2011.56.6.1983, 2011.
648 Suggett, D. J., Moore, C. M., Hickman, A. E., and Geider, R. J.: Interpretation of fast repetition
649 rate (FRR) fluorescence: signatures of phytoplankton community structure versus
650 physiological state, Mar Ecol Prog Ser, 376, 1-19, 10.3354/meps07830, 2009.
651 Sunda, W. G. and Huntsman, S. A.: Interrelated influence of iron, light and cell size on marine
652 phytoplankton growth, Nature, 390, 389-392, 10.1038/37093, 1997.
653 Sverdrup, H. U.: On conditions for the vernal blooming of phytoplankton, Journal du Conseil
654 International pour l'Exploration de la Mer, 18, 287-295, 1953.
655 Swart, S., Chang, N., Fauchereau, N., Joubert, W. R., Lucas, M., Mtshali, T., Roychoudhury,
656 A., Tagliabue, A., Thomalla, S., Waldron, H. N., and Monteiro, P. M. S.: Southern Ocean
657 Seasonal Cycle Experiment 2012: Seasonal scale climate and carbon cycle links, S Afr J Sci,
658 108, 11-13, 10.4102/sajs.v108i3/4.1089, 2012.
659 Swart, S., Speich, S., Ansorge, I. J., and Lutjeharms, J. R. E.: An altimetry-based gravest
660 empirical mode south of Africa: 1. Development and validation, J Geophys Res, 115, C03002,
661 10.1029/2009JC005299, 2010.
662 Swart, S., Thomalla, S. J., and Monteiro, P. M. S.: The seasonal cycle of mixed layer dynamics
663 and phytoplankton biomass in the Sub-Antarctic Zone: A high-resolution glider experiment,
664 Journal of Marine Systems, 147, 103-115, 10.1016/j.jmarsys.2014.06.002, 2015.

665 Tagliabue, A., Sallée, J.-B., Bowie, A. R., Lévy, M., Swart, S., and Boyd, P. W.: Surface-water
666 iron supplies in the Southern Ocean sustained by deep winter mixing, Nature Geoscience, 7,
667 314-320, 10.1038/ngeo2101, 2014.
668 Thomalla, S. J., Fauchereau, N., Swart, S., and Monteiro, P. M. S.: Regional scale
669 characteristics of the seasonal cycle of chlorophyll in the Southern Ocean, Biogeosciences, 8,
670 2849-2866, 10.5194/bg-8-2849-2011, 2011.
671 Thomalla, S. J., Moutier, W., Ryan-Keogh, T. J., Gregor, L., and Schütt, J.: An optimized
672 method for correcting fluorescence quenching using optical backscattering on autonomous
673 platforms, Limnology and Oceanography Methods, In Press, 2017.
674 Thomalla, S. J., Racault, M.-F., Swart, S., and Monteiro, P. M. S.: High-resolution view of the
675 spring bloom initiation and net community production in the Subantarctic Southern Ocean
676 using glider data, ICES J Mar Sci, 72, 1999-2020, 10.1093/icesjms/fsv105, 2015.
677 Welschmeyer, N. A.: Fluorometric analysis of chlorophyll-*a* in the presence of chlorophyll-b
678 and pheopigments, Limnol Oceanogr, 39, 1985-1992, 10.4319/lo.1994.39.8.1985, 1994.
679 Westberry, T., Behrenfeld, M. J., Siegel, D. A., and Boss, E.: Carbon-based primary
680 productivity modeling with vertically resolved photoacclimation, Global Biogeochemical
681 Cycles, 22, GB2024, 10.1029/2007GB003078, 2008.
682 Westberry, T. K., Schultz, P., Behrenfeld, M. J., Dunne, J. P., Hiscock, M. R., Maritorena, S.,
683 Sarmiento, J. L., and Siegel, D. A.: Annual cycles of phytoplankton biomass in the subarctic
684 Atlantic and Pacific Ocean, Global Biogeochemical Cycles, 30, 175-190,
685 10.1002/2015GB005276, 2016.
686 Wolters, M.: Quickchem Method 31-114-27-1-D - Silicate in Brackish or Seawater, Lachat
687 Instruments, 2002.
688

Biogeosciences Discuss., https://doi.org/10.5194/bg-2017-551
Manuscript under review for journal Biogeosciences
Discussion started: 8 January 2018

689 **Table 1: Locations of experiments conducted during the cruise along with details of the**

690 **initial set up conditions.**

Experiment	Experiment 1	Experiment 2	Experiment 3
	'Early Summer'	'Mid-Summer'	'Late Summer'
Run time (h)	168	168	144
Initiation Date	08/12/2015	05/01/2016	08/02/2016
Latitude (°S)	-42.693	-42.693	-43.000
Longitude (°E)	8.738	8.737	8.500
Collection Depth (m)	30	35	35
Sunrise:Sunset (GMT)	03:30 – 18:30	04:00 – 19:00	04:40 – 18:40
Chl-a (µg L^{-1})	0.97	0.84	0.90
Nitrate (µM)	10.60	12.80	18.25
Silicate (µM)	1.46	1.43	1.39
Phosphate (µM)	0.88	0.76	0.45
DFe (nM)	0.16	0.17	0.05
F_v/F_m	0.19±0.06	0.30±0.02	0.26±0.01
σ_{PSII} (nm^{-2})	14.79±2.46	6.45±0.40	7.08±0.48
MLD (m)	33.77	56.96	43.32
Salinity	33.87	33.70	34.11
Temp (°C)	10.80	10.44	10.80
% Light Depth	14.83	11.59	10.66

691

692

Biogeosciences Discuss., https://doi.org/10.5194/bg-2017-551
Manuscript under review for journal Biogeosciences
Discussion started: 8 January 2018

693 **Table 2: Net growth rates calculated from chlorophyll accumulation (μ^{Chl}) and nitrate**

694 **drawdown ($\Delta(NO_3^-)$) over the full experimental running time (t = 168, 168, 144 h).**

695 **Shown are averages with ± standard deviations, where n = 5.**

Experiment	μ^{Chl} (d^{-1}) 0 - end		$\Delta(NO_3^-)$ (µmol L^{-1} d^{-1})	
	+ Fe	Control	+ Fe	Control
1	0.28±0.02	0.27±0.02	0.98±0.005	0.82±0.07
2	0.23±0.01	0.11±0.01	4.29±0.43	3.19±0.54
3	0.23±0.01	0.09±0.01	0.78±0.11	0.91±0.15

696

Biogeosciences Discuss., https://doi.org/10.5194/bg-2017-551
Manuscript under review for journal Biogeosciences
Discussion started: 8 January 2018

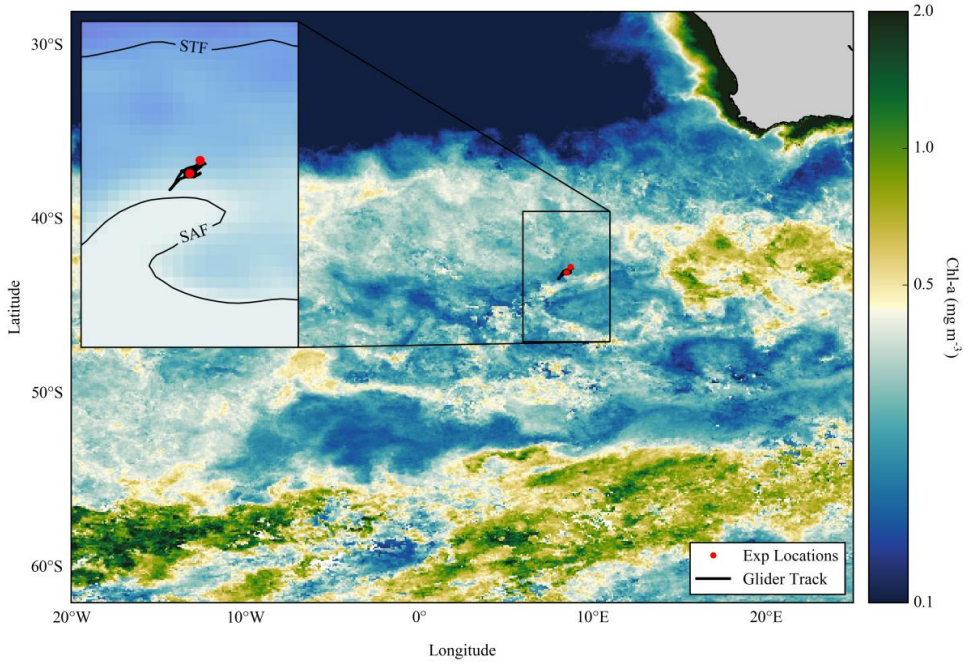

Figure 1: Composite map of MODIS (8-day, 9 km) derived chlorophyll-a (mg m^{-3}) from December 2015 to February 2016 for the Atlantic sector of the Southern Ocean, with locations of nutrient addition incubation experiments and the glider track. Inset composite map of MADT from the CLS/AVISO product (Rio et al., 2011) from December 2015 to February 2016 with boundary definitions of sub-tropical front (STF) and sub-Antarctic front (SAF) (Swart et al., 2010), with locations of experiments and glider track.

Biogeosciences Discuss., https://doi.org/10.5194/bg-2017-551
Manuscript under review for journal Biogeosciences
Discussion started: 8 January 2018

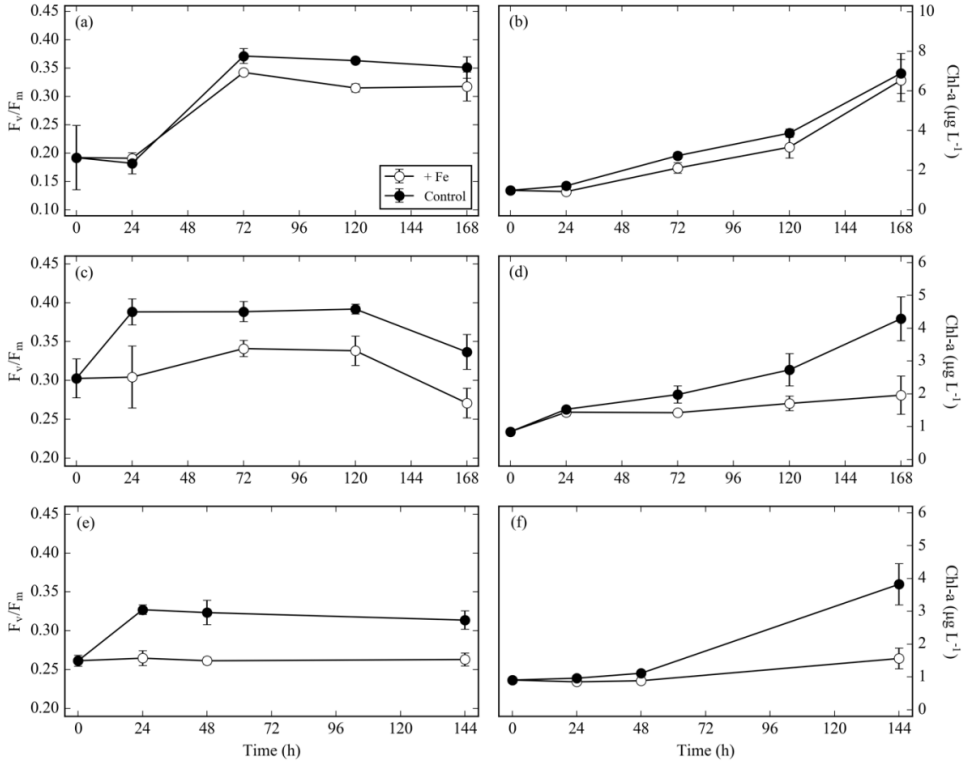

Figure 2: F_v/F_m (a, c, e) and chlorophyll-a (Chl-a) responses (μg L^{-1}) (b, d, f), from the control and Fe addition treatments of experiments initiated in the sub-Antarctic zone over early summer (a, b), mid-summer (c, d), and late summer (e, f). Displayed here are averages with ± standard deviations (*n* = 3 for all time points, except the end time point where *n* = 5). Please note the different scales in panels a and b.

Biogeosciences Discuss., https://doi.org/10.5194/bg-2017-551
Manuscript under review for journal Biogeosciences
Discussion started: 8 January 2018

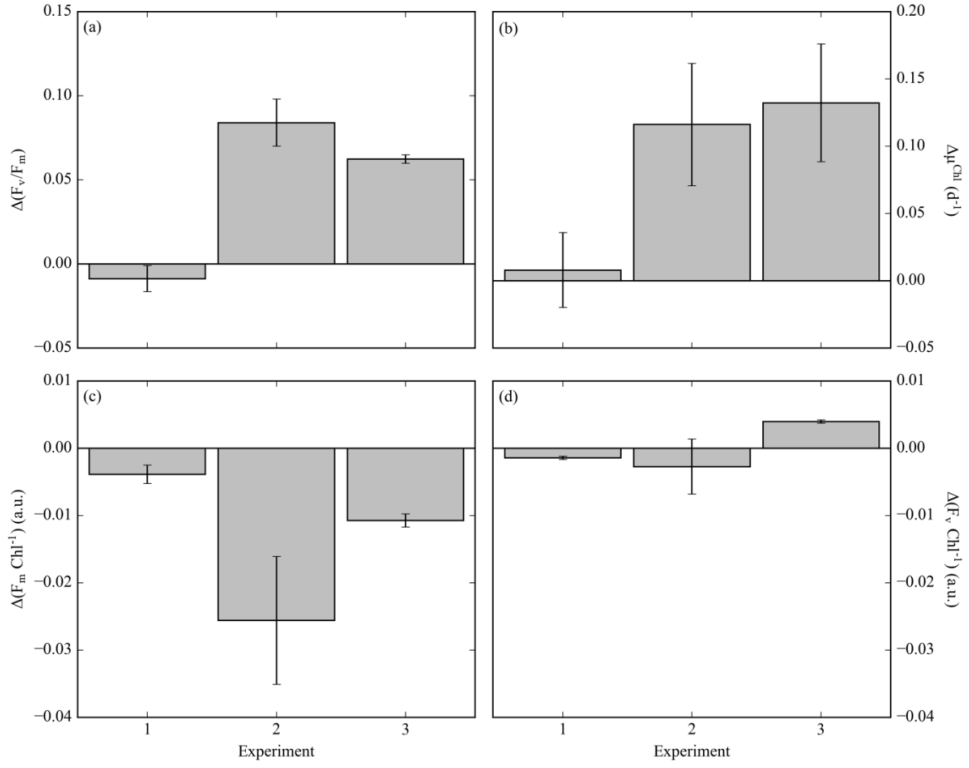

Figure 3: (a) The difference in F_v/F_m between the Fe treatment and control treatment ($\Delta(F_v/F_m)$) at the 24 h time point for experiments initiated in early summer (experiment 1), mid-summer (experiment 2) and late summer (experiment 3). (b) The difference in chlorophyll derived net growth rates ($\Delta\mu^{Chl}$ (d^{-1})), where t = 168, 168 and 144 h. (c) The change in chlorophyll normalised maximum fluorescence, (ΔF_m Chl^{-1}). (d) The change in chlorophyll normalised variable fluorescence, (ΔF_v Chl^{-1}). Displayed here are averages with ± standard deviations (n = 3 – 5).

Biogeosciences Discuss., https://doi.org/10.5194/bg-2017-551
Manuscript under review for journal Biogeosciences
Discussion started: 8 January 2018

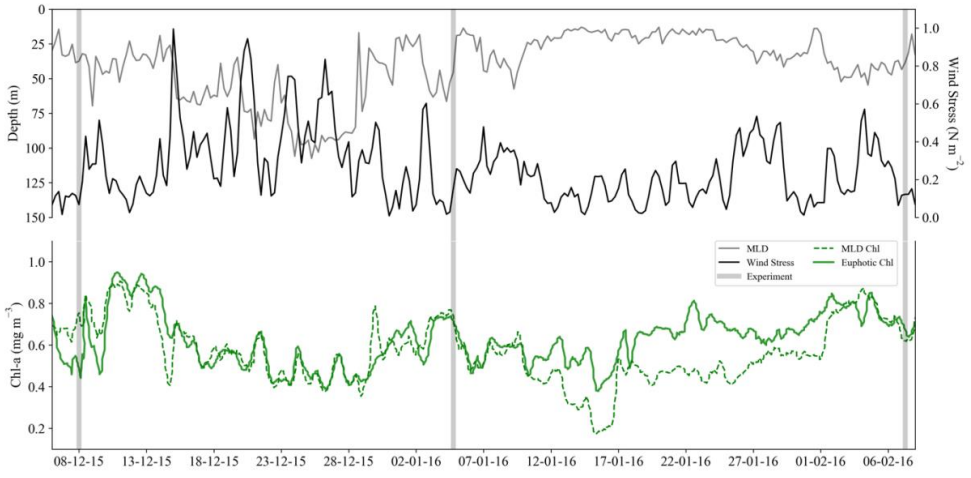

Figure 4: Time series from 6th December 2015 to 8th February 2016 of (a) surface wind stress (N m^{-2}), mixed layer depth (MLD, m) where ΔT_{10m} = 0.2°C, and (b) mean chlorophyll-a concentration (mg m^{-3}) from the MLD and the euphotic zone. Experiment initiation dates are overlaid in grey bars.